Amino Acids (2014) 46:2693–2704
DOI 10.1007/s00726-014-1826-8

ORIGINAL ARTICLE

The regulatory peptide apelin: a novel inhibitor of renal interstitial fibrosis

Li-Yan Wang · Zong-Li Diao · Dong-Liang Zhang · Jun-Fang Zheng · Qi-Dong Zhang · Jia-Xiang Ding · Wen-Hu Liu

Received: 23 May 2014 / Accepted: 14 August 2014 / Published online: 28 August 2014

Abstract Epithelial–mesenchymal transition (EMT) of tubular epithelial cells is a key event in renal interstitial fibrosis and the progression of chronic kidney disease (CKD). Apelin is a regulatory peptide involved in the regulation of normal renal hemodynamics and tubular functions, but its role in renal fibrosis remains unknown. In this study, we examined the inhibitory effects of apelin on transforming growth factor-β1 (TGF-β1)-induced EMT in HK-2 cells, and evaluated its therapeutic efficacy in mice with complete unilateral ureteral obstruction (UUO). In vitro, apelin inhibited TGF-β1-mediated upregulation of α-smooth muscle actin (α-SMA) and downregulation of E-cadherin. Increased levels of phosphorylated Smad-2/3 and decreased levels of Smad7 in TGF-β1-stimulated cells were reversed by apelin co-treatment. In the UUO model, administration of apelin significantly attenuated renal interstitial fibrosis, as evidenced by the maintenance of E-cadherin and laminin expression, and markedly suppressed expression of α-SMA, TGF-β1 and its type I receptor, as well as interstitial matrix components. Interestingly, in UUO mice, there was a reduction in the plasma level of apelin, which was compensated by upregulation of APJ expression in the injured kidney. Exogenous supplementation of apelin normalized the level of plasmatic apelin and renal APJ. In conclusion, our study provides the first evidence that apelin is able to ameliorate renal interstitial fibrosis by suppression of tubular EMT through a Smad-dependent mechanism. The apelinergic system itself may promote some compensatory response in the renal fibrotic process. These results suggest that apelin has potential renoprotective effects and may be an effective agent for retarding CKD progression.

Keywords Apelin · Chronic kidney disease · Fibrosis · Tubule cells

Introduction

It is generally recognized that the prevalence of chronic kidney disease (CKD) is increasing worldwide (Coresh et al. 2007). Renal interstitial fibrosis is the common pathway for most forms of CKD, which progressively develops to end-stage renal disease (ESRD) irrespective of the underlying etiological factors (Wynn 2008). Accumulating evidence suggests that epithelial–mesenchymal transition (EMT) of tubular epithelial cells contributes significantly to the onset and pathogenesis of renal interstitial fibrosis (Liu 2004; Compagnone et al. 2012). During the process of EMT, tubular epithelial cells lose their epithelial markers and gain mesenchymal features, resulting in kidney tubule destruction, myofibroblast accumulation, and overproduction of interstitial matrix components (Lan 2003). Consequently, there is destruction of the integrity and function of nephrons. Of the many factors that trigger EMT, transforming growth factor-β1 (TGF-β1) is the major factor that mediates this process via numerous intracellular signal transduction

Electronic supplementary material The online version of this article (doi:10.1007/s00726-014-1826-8) contains supplementary material, which is available to authorized users.

L.-Y. Wang · Z.-L. Diao · D.-L. Zhang · Q.-D. Zhang · J.-X. Ding · W.-H. Liu (✉)
Department of Nephrology, Beijing Friendship Hospital, Capital Medical University, No. 95 Yong An Road, Xi Cheng District, Beijing 100050, China
e-mail: nephro@ccmu.edu.cn

J.-F. Zheng
Department of Biochemistry and Molecular Biology, Capital Medical University, Beijing 100069, China

pathways (Liu 2004). Despite the fact that EMT plays an important role in renal fibrosis, some studies have suggested that this pathological transition may be reversible (Yang and Liu 2002; Zeisberg et al. 2003). Therefore, it is important to study which interventions can potentially reverse or inhibit EMT in kidneys and retard CKD progression.

Apelin is the endogenous peptide ligand for the previously orphaned G protein-coupled APJ receptor (Cui et al. 2010). Both apelin and APJ are distributed in a wide variety of tissues including the central nervous system, heart, lungs, and kidneys (Kawamata et al. 2001; Medhurst et al. 2003). Intense research of the apelinergic system has revealed its involvement in the regulation of cardiovascular function, hemodynamic homeostasis, immune responses, brain signaling, human immunodeficiency virus infection, and insulin secretion (Cayabyab et al. 2000; Berry et al. 2004; Sorhede et al. 2005). Furthermore, there is growing evidence that apelin plays a role in tissue fibrosis. Administration of apelin can attenuate cardiac hypertrophy and fibrogenesis induced by pressure overload. These antifibrotic effects of apelin are mediated through the inhibition of TGF-β-induced phenotypic switching of cardiac fibroblasts to myofibroblasts (Pchejetski et al. 2012). Conversely, in chronic liver disease, the hepatic apelin system has been identified as an important mediator in the initiation and maintenance of inflammatory and fibrogenic processes (Melgar-Lesmes et al. 2010). As a novel regulator, apelin has complex effects on renal hemodynamics and tubular functions (Hus-Citharel et al. 2008), but its role has not been elucidated in renal fibrosis. Previous studies have shown altered levels of apelin either in the plasma or kidneys of CKD patients, and upregulation of the apelinergic system may exert some antifibrotic renal protection (El-Shehaby et al. 2010; Nishida et al. 2012). However, it is unknown whether the beneficial effects of apelin are related to inhibition of tubular EMT.

In the present study, we examined the antifibrotic effects of apelin in TGF-β1-induced EMT of human proximal tubular epithelial cells in vitro and a mouse model of tubulointerstitial fibrosis induced by unilateral ureteral obstruction (UUO) in vivo. Moreover, we elucidated whether the effects of apelin are mediated by interference of TGF-β1/Smad pathways that have been demonstrated to be important signaling pathways in tubular EMT and renal interstitial fibrosis.

Materials and methods

Cell culture and treatments

HK-2 cells were obtained from the American Type Culture Collection (Manassas, VA). The cells were cultured in Dulbecco's modified Eagle medium (Sigma-Aldrich, St. Louis, MO) supplemented with 5 % fetal bovine serum (Gibco, Grand Island, NY) as described previously (Sun et al. 2009). After serum starvation overnight, HK-2 cells were incubated with various concentrations of apelin-13 (10^{-8}, 10^{-7} and 10^{-6} mol/L; Bachem, Merseyside, UK) in the absence or presence of TGF-β1 (2 ng/ml; R&D Systems, Minneapolis, MN) for 48 h unless indicated otherwise. The cells were then collected for various analyses.

Animal models

Seven-week-old male C57Bl/6j mice (weighing approximately 20–22 g) were obtained from the Institute of Laboratory Animal Science, Chinese Academy of Medical Sciences (Beijing, China). Animals were randomly assigned to four groups ($n = 5$): (1) sham + vehicle, (2) UUO + vehicle, (3) UUO + apelin-13, and (4) sham + apelin-13. UUO was carried out using an established protocol (Jones et al. 2009). Briefly, the mice were anaesthetized with sodium pentobarbital (50 mg/kg body weight) and the left ureter was double ligated. Sham-operated mice had their ureters exposed, but not ligated. Starting the day of surgery, the mice received apelin-13 (dissolved in PBS) at a dosage of 0.1 μmol/kg body weight or the vehicle alone by intraperitoneal injection every 24 h. After 2 weeks, the mice were killed and their kidney tissues were removed for various analyses. The animal protocol conformed to the Guide for the Care and Use of Laboratory Animals published by the US National Institutes of Health and was approved by the Animal Experimentation Ethics Committee of Capital Medical University.

Immunofluorescence staining

Indirect immunofluorescence staining was carried out as described previously (Li et al. 2003). Briefly, cells cultured on coverslips were fixed with 4 % paraformaldehyde and incubated with specific primary antibodies against α-SMA (ab5694; Abcam, Cambridge, MA) or E-cadherin (sc-28644; Santa Cruz Biotechnology, Santa Cruz, CA). Frozen sections of kidney tissues were cut at 5 μm, fixed with cold acetone, and then incubated with primary antibodies against α-SMA, E-cadherin (3195, Cell Signaling Technology, Beverly, MA), or laminin (ab30320; Abcam). Then, the cells and cryosections were stained with secondary antibodies labeled with Alexa Fluor 488 or 555. Some samples were double stained with 4′,6-diamidino-2-phenylindole–HCl to visualize nuclei. Images of the cells and cryosections were obtained by confocal laser scanning microscopy (TCS SP5; Leica, Mannheim, Germany).

Semiquantitative assessment of renal fibrosis

To evaluate the extent of fibrosis, 3 μm sections of paraffin-embedded kidney tissues were subjected to Masson's

trichrome staining (MTS) by routine procedures (He et al. 2009). Stained sections were examined under an Eclipse E600 epifluorescence microscope equipped with a digital camera (Nikon, Melville, NY). The severity of renal fibrotic lesions was defined as the percentage of MTS-positive areas and analyzed by the Image Acquisition and Analysis Software LabWorks (Ultra-Violet Products, Cambridge, UK). For each sample, we analyzed five randomly selected non-overlapping fields.

Immunohistochemistry

Paraffin Sections (5 μm thickness) of kidney tissues were incubated with primary antibodies against fibronectin (ab2413; Abcam), collagen I (ab34710; Abcam), or APJ (ABD43; Millipore, Billerica, MA) overnight at 4 °C. Staining was performed using an ABC ELITE kit (Vector Laboratories, Burlingame, CA) including biotinylated secondary antibodies according to the manufacturer's instructions. Sections that were stained with secondary antibodies alone were confirmed to be negative. Image acquisition was performed using the analysis system described above.

Quantitative real-time PCR

Total RNA was isolated with Trizol reagent (Invitrogen, Ontario, Canada) and methyl trichloride according to the manufacturer's instructions. RNA concentration and quality were checked by spectrophotometry. First-strand cDNA was synthesized from 2 μg RNA by reverse transcription using AMV-RT (Promega, Madison, WI) and random primers at 42 °C for 30 min. Quantitative RT-PCR was performed on an ABI PRISM 7000 sequence detection system (Applied Biosystems, Foster City, CA). The 25 μl reaction mixture included 12.5 μl 2× SYBR Green PCR Master Mix (Applied Biosystems), 5 μl diluted cDNA (1:10), and 0.5 μM sense and antisense primers. The primers were designed using Primer Express software v.2.0 (Applied Biosystems) and their sequences are provided in Supplementary Table 1. Amplification was carried out under the following conditions: initial denaturation for 10 min at 95 °C, denaturation for 10 s at 95 °C, annealing for 30 s at an optimal temperature for each cDNA, and extension for 30 s at 72 °C. The mRNA levels of target genes were calculated after normalization to glyceraldehyde-3-phosphate dehydrogenase (GAPDH) mRNA.

Western blot analysis

Preparation of whole cell lysates and kidney tissue homogenates, and the immunoblotting assay were performed according to previously described procedures (Yang and Liu 2002). The primary antibodies were obtained from the following sources: anti-α-SMA (ab5694), anti-TβRI (ab31013), and anti-TGF-β1 (ab53169; Abcam); anti-E-cadherin (3195), anti-p-Smad2 (Ser465/467)/Smad3 (Ser423/425) (8828), anti-Smad2/3 (8685), anti-p-Smad-2 (Ser465/467) (3108), and anti-Smad-2 (5339) (Cell Signaling Technology); anti-Smad-7 (sc-11392; Santa Cruz Biotechnology); anti-APJ (ABD43; Millipore).

Enzyme-linked immunosorbent assay (ELISA)

The plasma levels of apelin in mice were evaluated by ELISA. Venous blood samples were collected in EDTA-/acetic acid-containing tubes and centrifuged at 5,000 rpm for 15 min at 4 °C. The plasma was collected and frozen at −70 °C until analysis. Apelin assays were performed using an apelin-36 microplate ELISA kit (Phoenix Pharmaceuticals, Karlsruhe, Germany) according to the manufacturer's instructions. The antibody used in this apelin assay cross-reacts with mouse apelin-36, the precursor of all biologically active forms of apelin.

Statistical analyses

All data are expressed as the mean ± standard deviation (SD). Statistical analyses were performed using SPSS version 13.0 software. Comparisons between groups were made using one-way analysis of variance followed by the Student–Newman–Keuls test. $P < 0.05$ was considered to be statistically significant.

Results

Apelin inhibits TGF-β1-mediated tubular EMT in vitro

First, to obtain direct evidence that apelin is able to target tubular EMT, we used an in vitro cell culture system in which human proximal tubule epithelial cells (HK-2) were induced to undergo EMT by TGF-β1 (Yang and Liu 2002). After treatment with TGF-β1, immunofluorescence staining showed that HK-2 cells began to lose the epithelial adhesion receptor E-cadherin and gained the mesenchymal marker α-smooth muscle actin (α-SMA). However, simultaneous treatment with apelin-13 abolished TGF-β1-induced α-SMA expression and assembly, and restored E-cadherin expression (Fig. 1a). Similarly, Western blot analyses revealed that the decreased expression of E-cadherin and increased expression of α-SMA after TGF-β1 exposure were significantly reversed by apelin-13 in a dose-dependent manner (Fig. 1b–d). However, when HK-2 cells were exposed to the APJ antagonist F13A, the inhibitory effects of apelin on EMT were almost completely counteracted (Fig. S1 a–c).

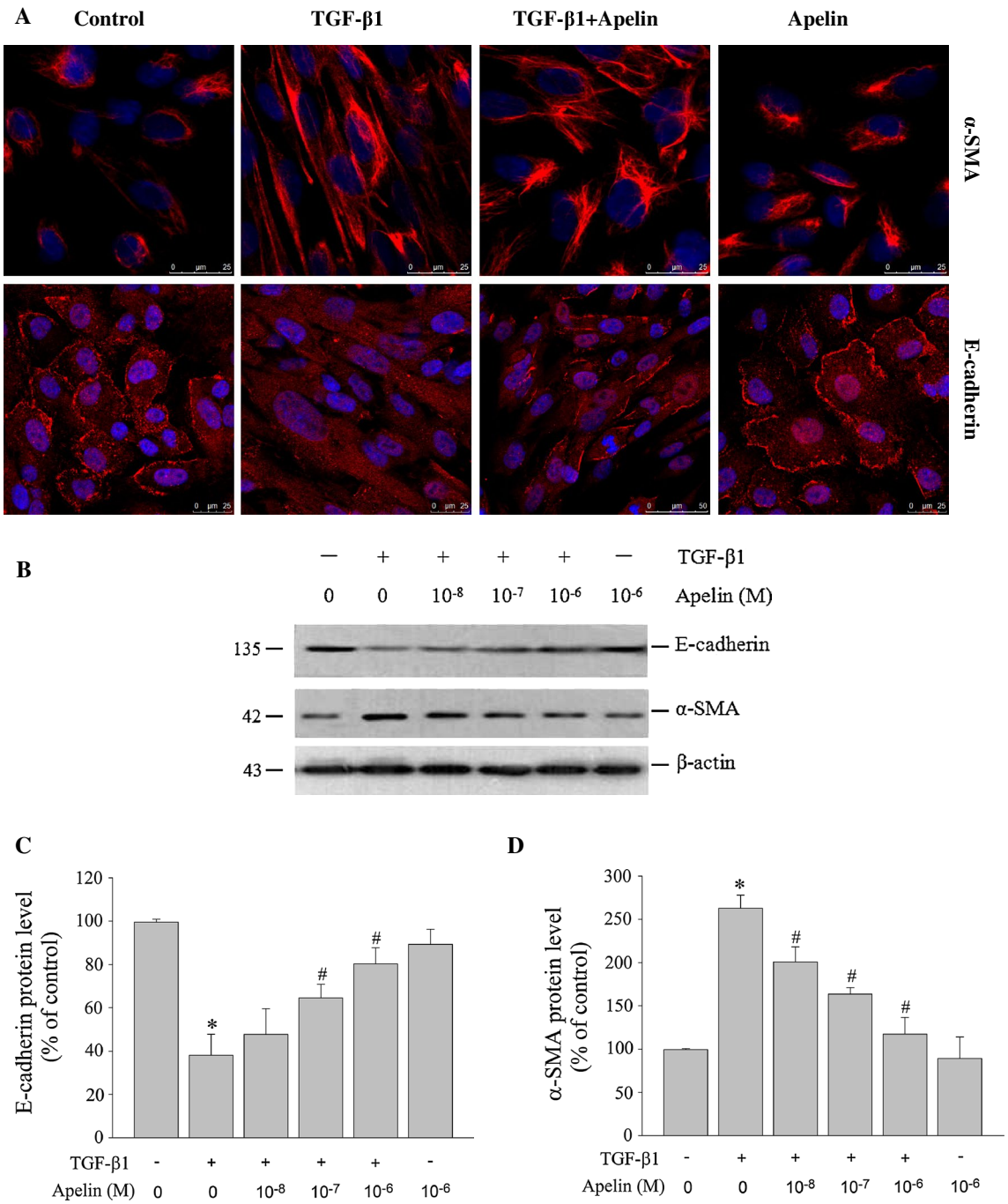

Fig. 1 Apelin blocks TGF-β1-mediated epithelial to mesenchymal transition (EMT) in vitro. Human proximal tubular epithelial cells (HK-2) were treated with 2 ng/ml TGF-β1 in the presence or absence of various concentrations of apelin-13 as indicated for 48 h. **a** Immunofluorescence staining showed that apelin-13 (10^{-6} mol/L) abolished TGF-β1-induced α-SMA assembly and preserved E-cadherin integrity. **b** Western blotting showed that treatment with apelin-13 (10^{-8}, 10^{-7} and 10^{-6} mol/L) reversed the increased expression of α-SMA and decreased expression of E-cadherin induced by TGF-β1 in a dose-dependent manner. Cell lysates were immunoblotted with antibodies against E-cadherin, α-SMA, or β-actin. **c**, **d** Densitometric analysis of E-cadherin and α-SMA protein levels. Results are presented as percentages of control values after normalization to β-actin and are the means ± SD of three independent experiments. $^{*}P < 0.05$, compared with control groups. $^{\#}P < 0.05$, compared with TGF-β1-stimulated groups; $n = 5$ in each group

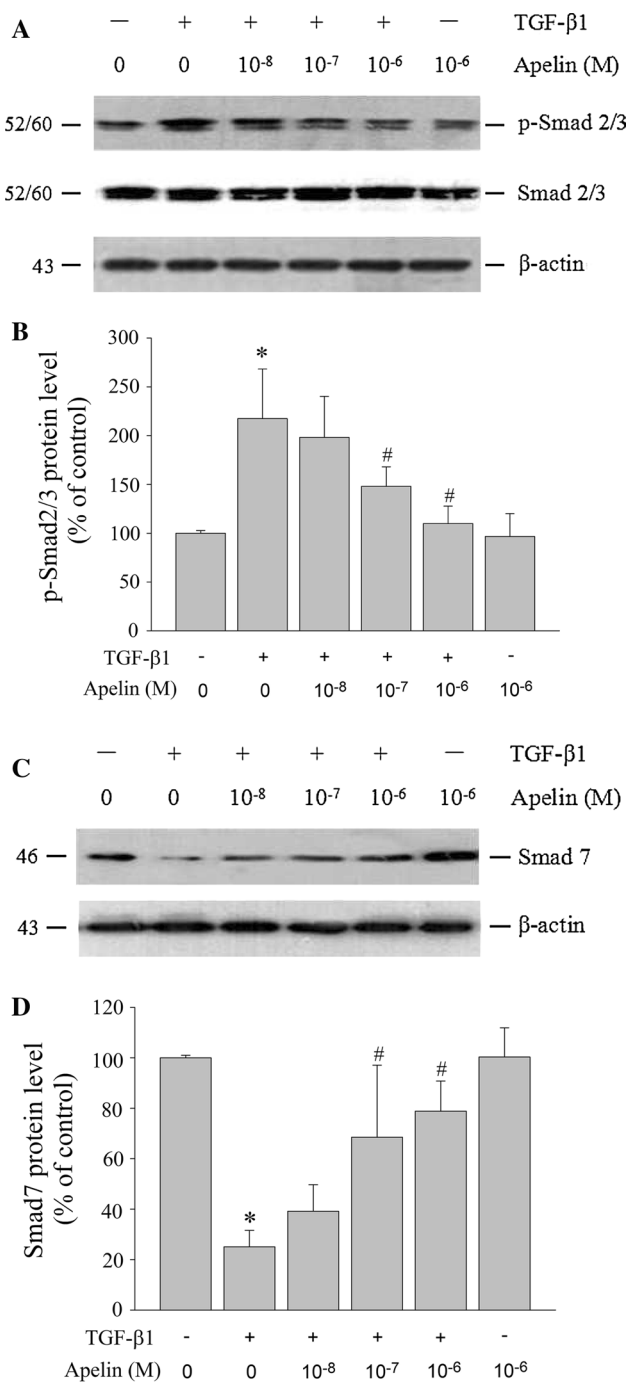

Fig. 2 Apelin inhibits the TGF-β1-mediated increase of phosphorylated Smad2/3 and decrease of Smad7 in vitro. Human proximal tubular epithelial cells (HK-2) were treated with 2 ng/ml TGF-β1 in the presence or absence of apelin-13 (10^{-8}, 10^{-7} and 10^{-6} mol/L) for 48 h. **a** Western blotting showed that apelin-13 inhibited TGF-β1-induced Smad2/3 phosphorylation. Cell lysates were immunoblotted with antibodies against phosphorylated Smad2/3 (p-Smad2/3), total Smad2/3, or β-actin. **c** Apelin-13 reversed the decreased expression of Smad7 induced by TGF-β1. Cell lysates were immunoblotted with antibodies against Smad7 or β-actin. **b**, **d** Densitometric analysis of p-Smad2/3 and Smad7 protein levels. Results are presented as percentages of control values after normalization to β-actin and are the means ± SD of three independent experiments. $^{*}P < 0.05$, compared with control groups. $^{\#}P < 0.05$, compared with TGF-β1-stimulated groups; $n = 5$ in each group

Apelin inhibits TGF-β1-mediated EMT by a Smad-dependent mechanism

To better understand the molecular mechanism of the inhibitory effects of apelin in EMT, we investigated the possible involvement of key TGF-β1/Smad pathways. The results demonstrated that there was no significant change between each group in terms of Smad2/3 expression, but the level of phosphorylated Smad2/3 was markedly increased after treatment with TGF-β1. Conversely, 10^{-7} and 10^{-6} M apelin-13 significantly attenuated TGF-β1-induced upregulation of phosphorylated Smad2/3 (Fig. 2a, b). Moreover, the expression of Smad7, a negative regulator of TGF-β1/Smad signaling, was reduced after TGF-β1 stimulation, whereas administration of apelin-13 increased its expression (Fig. 2c, d).

Apelin attenuates TGF-β1-induced upregulation of APJ expression in vitro

To further explore whether the apelinergic system has a compensatory response during EMT, we measured mRNA expression of apelin and APJ in HK-2 cells after exposure to TGF-β1. As a result, we observed strong upregulation of APJ. The amount of APJ transcripts was around six-fold higher in TGF-β1-treated cells than that in controls (Fig. 3a). Apelin showed a similar trend of mRNA expression, but the difference did not reach statistical significance (Fig. 3b). Remarkably, co-treatment with apelin-13 blunted the increase of APJ mRNA expression in a dose-dependent manner, resulting in APJ transcripts declining to near normal levels (Fig. 3a).

Apelin ameliorates renal interstitial fibrosis in the UUO model

Because apelin was able to block the fibrogenic action in vitro, we tested its therapeutic efficacy to mitigate renal fibrosis after injury in vivo. To this end, apelin-13 was administrated daily to UUO mice. Figure 4a shows the representative micrographs of kidney sections subjected to MTS of various groups. At 14 days after UUO, tubular atrophy and increased interstitial fibrosis were seen in the ligated kidney treated with the vehicle alone, whereas the fibrotic lesion was significantly attenuated in the ligated kidney treated with apelin-13. In sham-operated kidneys treated with the vehicle or apelin-13, the tubulointerstitium was normal (Fig. 4a, b). However, the injection of F13A suppressed the antifibrotic effects of apelin. The fibrotic

lesion of ligated kidney in UUO mice treated with apelin-13 plus F13A was as serious as in UUO mice treated with vehicle (Fig. S1 d, e).

We further examined the expression of major interstitial matrix components by RT-PCR. As shown in Fig. 4c, markedly increased levels of collagen I, collagen III, and fibronectin mRNAs were found in the ligated kidney compared with those in the sham control. Similarly, apelin-13 treatment significantly decreased the transcripts of these interstitial matrix genes. Immunohistochemical staining for fibronectin and collagen I produced results consistent with those of RT-PCR analyses (Fig. 4d, e).

Apelin inhibits the expression of EMT markers in the UUO model

We next examined the expression of E-cadherin, an epithelial marker, and the molecular hallmark of myofibroblasts, α-SMA. As shown in Fig. 5, ureteral obstruction induced suppression of E-cadherin and dramatic upregulation of α-SMA, a shift that is in agreement with tubular EMT. It is interesting that administration of apelin-13 preserved E-cadherin expression and inhibited induction of α-SMA expression in the obstructed kidney as demonstrated by immunofluorescence staining and Western blot analysis (Fig. 5b–e). Laminin is a key component of the tubular basement membrane, and a decrease in its expression was noted in tubules of the ligated kidney, whereas apelin-13 treatment maintained laminin expression (Fig. 5a).

Apelin interferes with the TGF-β1/Smad pathway in the UUO model

As shown in the in vitro experiments, apelin inhibited EMT by disrupting the TGF-β1/Smad pathway. Therefore, we determined whether apelin influenced the expression of TGF-β1 and its type I receptor (TβR-I) as well as downstream Smad signaling molecules in the UUO model. Western blotting indicated a four- and fivefold increase of TGF-β1 and TβR-I in the obstructed kidney compared with that in the sham control, respectively. However, apelin-13 treatment significantly inhibited the upregulation of TGF-β1 and TβR-I, which was caused by ureteral obstruction (Fig. 6a, b). Furthermore, we observed that the level of phosphorylated Smad2 was increased in the UUO kidney, whereas apelin-13 markedly attenuated this increase after 14 days of treatment (Fig. 6c, d).

The apelinergic system promotes a compensatory response in the UUO model

Considering that the expression of APJ was upregulated in HK-2 cells during EMT, we examined compensatory

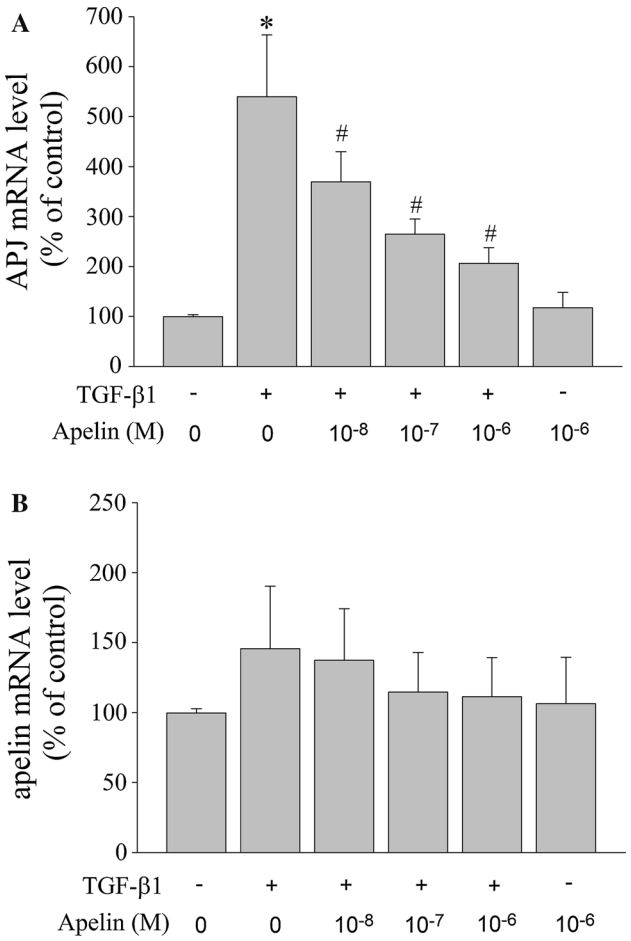

Fig. 3 Apelin suppresses TGF-β1-mediated upregulation of APJ, but does not affect apelin expression in tubular epithelial cells. Human proximal tubular epithelial cells (HK-2) were treated with 2 ng/ml TGF-β1 in the presence or absence of apelin-13 (10^{-8}, 10^{-7} and 10^{-6} mol/L) for 48 h. Total RNA was isolated and analyzed by quantitative RT-PCR to assess mRNA expression of APJ (**a**) and apelin (**b**). GAPDH mRNA expression was used as an internal control. Results are presented as percentages of control values and are the means ± SD of three independent experiments. $^{*}P < 0.05$, compared with control groups. $^{\#}P < 0.05$, compared with TGF-β1-stimulated groups; $n = 5$ in each group

responses for the apelinergic system in the renal fibrotic process in vivo. Interestingly, at 14 days after surgery, a significant decrease of apelin was observed in the plasma of UUO mice compared with that in sham controls (0.28 ± 0.10 vs. 0.69 ± 0.13 ng/ml, $P < 0.05$). Exogenous supplementation of apelin-13 normalized the plasma level of apelin in UUO mice (0.49 ± 0.07 ng/ml, $P < 0.05$). However, in sham mice, no significant changes were observed after treatment with apelin-13 (0.71 ± 0.11 ng/ml, $P = 0.79$).

In the ligated kidney, mRNA expression was significantly upregulated for APJ, but not apelin. However, apelin-13 administration markedly blunted this upregulation

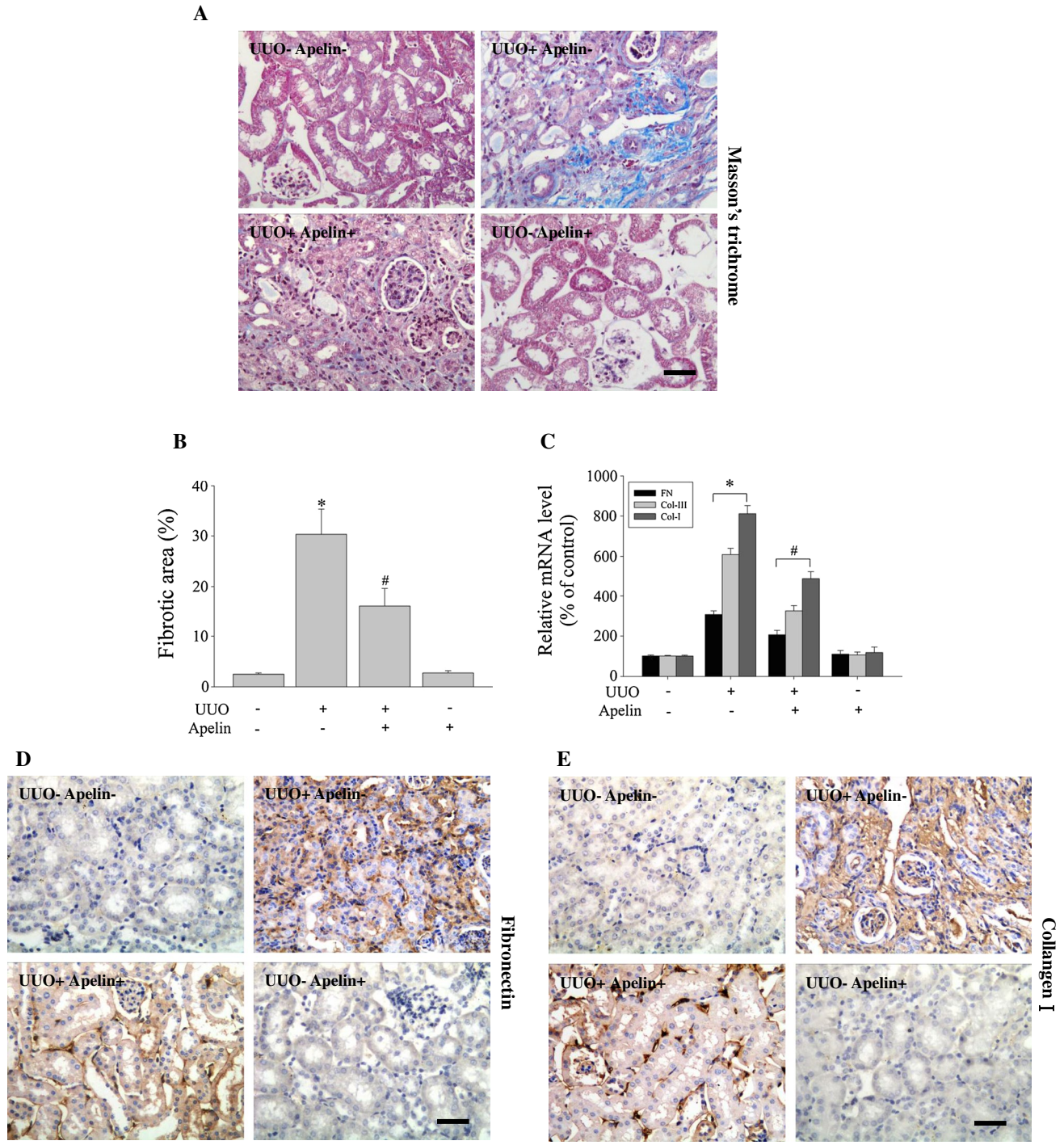

Fig. 4 Apelin attenuates renal interstitial fibrosis and decreases fibronectin and collagen deposition after ureteral obstruction. **a** Representative micrographs showing that apelin-13 ameliorated renal fibrotic lesions after obstructive injury. Kidney sections from various groups at 14 days after UUO were subjected to MTS. The dose of apelin-13 used was 0.1 μmol/kg body weight. *Scale bar*, 40 μm. **b** Quantitative determination of renal fibrotic lesions in various groups. Renal fibrotic lesions (defined as the percentage of the MTS-positive fibrotic area) were quantified by computer-aided morphometric analyses. **c** Quantitative RT-PCR analyses showed that apelin-13 inhibited renal expression of fibronectin, collagen I, and collagen III in the ligated kidney at 14 days after UUO. Results are presented as percentages of control values and are the means ± SD of five animals per group ($n = 5$). $^{*}P < 0.05$, compared with the UUO− apelin− group. $^{\#}P < 0.05$, compared with the UUO+ apelin− group. **d**, **e** Immunohistochemical staining showed that apelin-13 reduced fibronectin and collagen I deposition in the obstructed kidney. *Scale bar* 40 μm

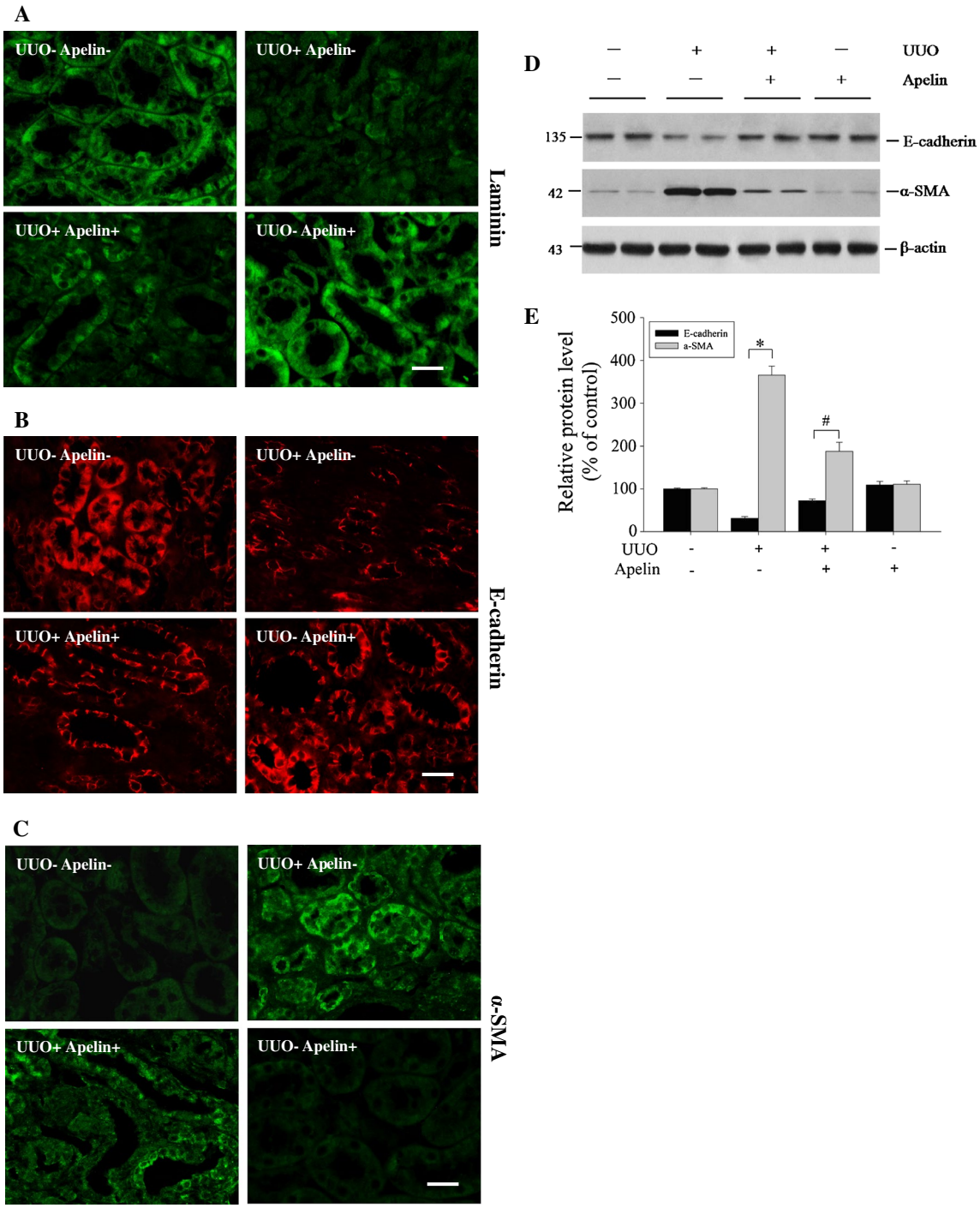

Fig. 5 Apelin maintains laminin in the tubular basement membrane, preserves epithelial E-cadherin, and inhibits α-SMA expression in the obstructed kidney. **a**–**c** Kidney sections from various groups at 14 days after UUO were stained with anti-laminin, anti-E-cadherin, or anti-α-SMA antibodies to outline the tubular basement membrane laminin, and to show the expression of the key epithelial protein E-cadherin and typical mesenchymal marker α-SMA. Representative micrographs are shown. *Scale bar* 20 μm. **d** Western blotting showed that apelin-13 reduced α-SMA expression and promoted E-cadherin expression in the ligated kidney. The dose of apelin-13 used was 0.1 μmol/kg body weight. Kidney homogenates were immunoblotted with antibodies against E-cadherin, α-SMA, or β-actin. **e** Densitometric analysis of E-cadherin and α-SMA protein levels. Results are presented as percentages of control values after normalization to β-actin and are the means ± SD of five animals per group ($n = 5$). $^{*}P < 0.05$, compared with the UUO− apelin− group. $^{\#}P < 0.05$, compared with the UUO+ apelin− group

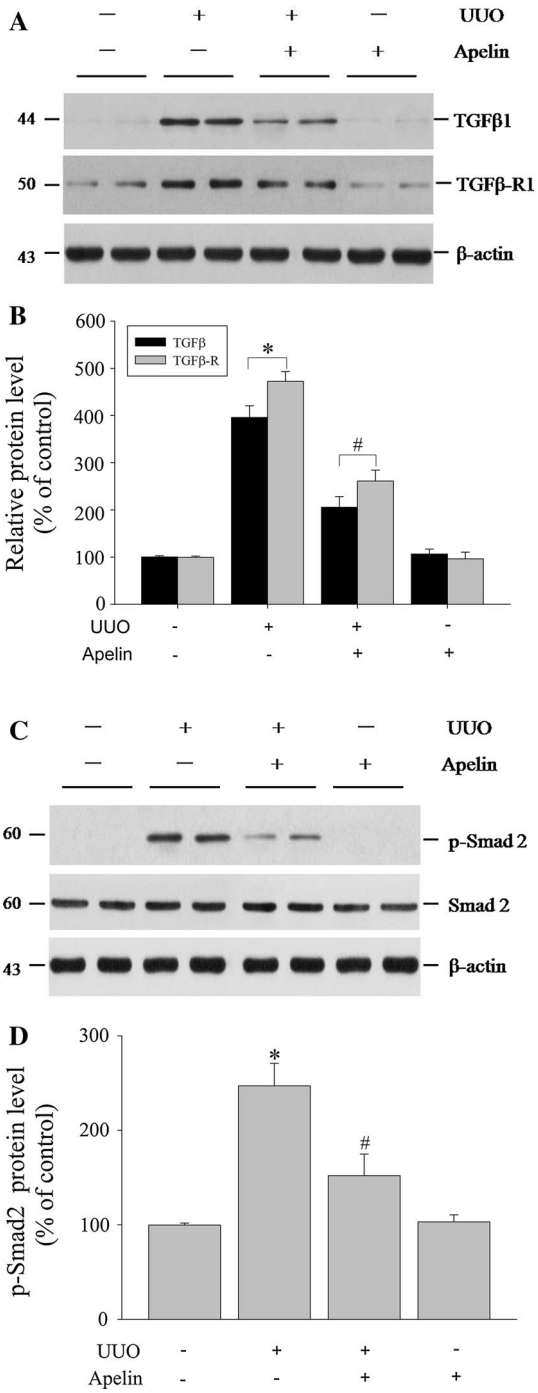

Fig. 6 Apelin inhibits the expression of both TGF-β1 and its type I receptor (TβR-I), and reduces the phosphorylated Smad2 level in the obstructed kidney. Western blotting and densitometric analysis demonstrated the protein levels of TGF-β1, TβR-I (**a**, **b**), and phosphorylated Smad2 (**c**, **d**) in the obstructed kidney of various groups at 14 days after UUO. The dose of apelin-13 used was 0.1 μmol/kg body weight. Kidney homogenates were immunoblotted with antibodies against TGF-β1, TβR-I, phosphorylated Smad2, total Smad2, or β-actin. Results are presented as percentages of control values after normalization to β-actin and are the means ± SD of five animals per group ($n = 5$). *$P < 0.05$, compared with the UUO− apelin− group. #$P < 0.05$, compared with the UUO+ apelin− group

(Fig. 7a, b). Immunoblotting of the APJ protein content in kidney homogenates showed the same trend (Fig. 7c, d). We also performed immunohistochemical staining of APJ to identify the localization of the apelinergic system in fibrotic kidneys. As shown in Fig. 7e, immunostaining of APJ was only slightly positive in the sham-operated kidney. However, in the ligated kidney, extensive immunostaining of APJ was found in the tubulointerstitium, which was more intense in severely fibrotic areas. However, treatment with apelin-13 attenuated the upregulated expression of APJ induced by ureteral obstruction.

Discussion

Progressive interstitial fibrosis is the predominant pathological feature of nearly all forms of CKD (Strutz 2009). Because current therapies only have limited efficacy, there is a need to identify new agents that target key molecular pathways involved in the pathogenesis of renal fibrosis to halt progression. Because apelin is a recently described endogenous peptide involved in the pathophysiological processes of heart and liver fibrosis, it is conceivable that apelin may also play some roles in renal fibrosis. In the present study, we demonstrated that apelin inhibited TGF-β1-induced EMT in proximal tubule epithelial cells, an important event in the pathogenesis of renal interstitial fibrosis. This effect was mediated by interference of the TGF-β1/Smad pathway, an important regulatory signaling pathway in tubular EMT and renal fibrotic processes. Furthermore, after UUO, a model with predominant tubulointerstitial lesions, APJ expression in the injured kidney underwent compensatory upregulation. Supplementation of apelin suppressed the expression of interstitial matrix components and ameliorated renal fibrogenesis. These results suggest that the novel peptide apelin may have potential therapeutic value for treatment of fibrotic kidney disease and retardation of CKD progression.

Both promotion and suppression of renal fibrosis are considered the consequences of dynamic processes that depend on fibroblast survival and the balance between extracellular matrix production and degradation. Increasing evidence indicates that tubular epithelial cells, the major constituents of renal parenchyma, are not bystanders but play a decisive role in the development of renal fibrosis (Liu 2006). Upon stimulation by profibrotic cues such as TGF-β1, tubular epithelial cells undergo EMT, a phenotypic conversion process that leads to the generation of matrix-producing interstitial fibroblasts and myofibroblasts. Therefore, inhibition of tubular EMT is an important target for treatment of renal fibrosis. The success of an agent to inhibit EMT is defined as the suppression of mesenchymal markers and preservation of important epithelial proteins,

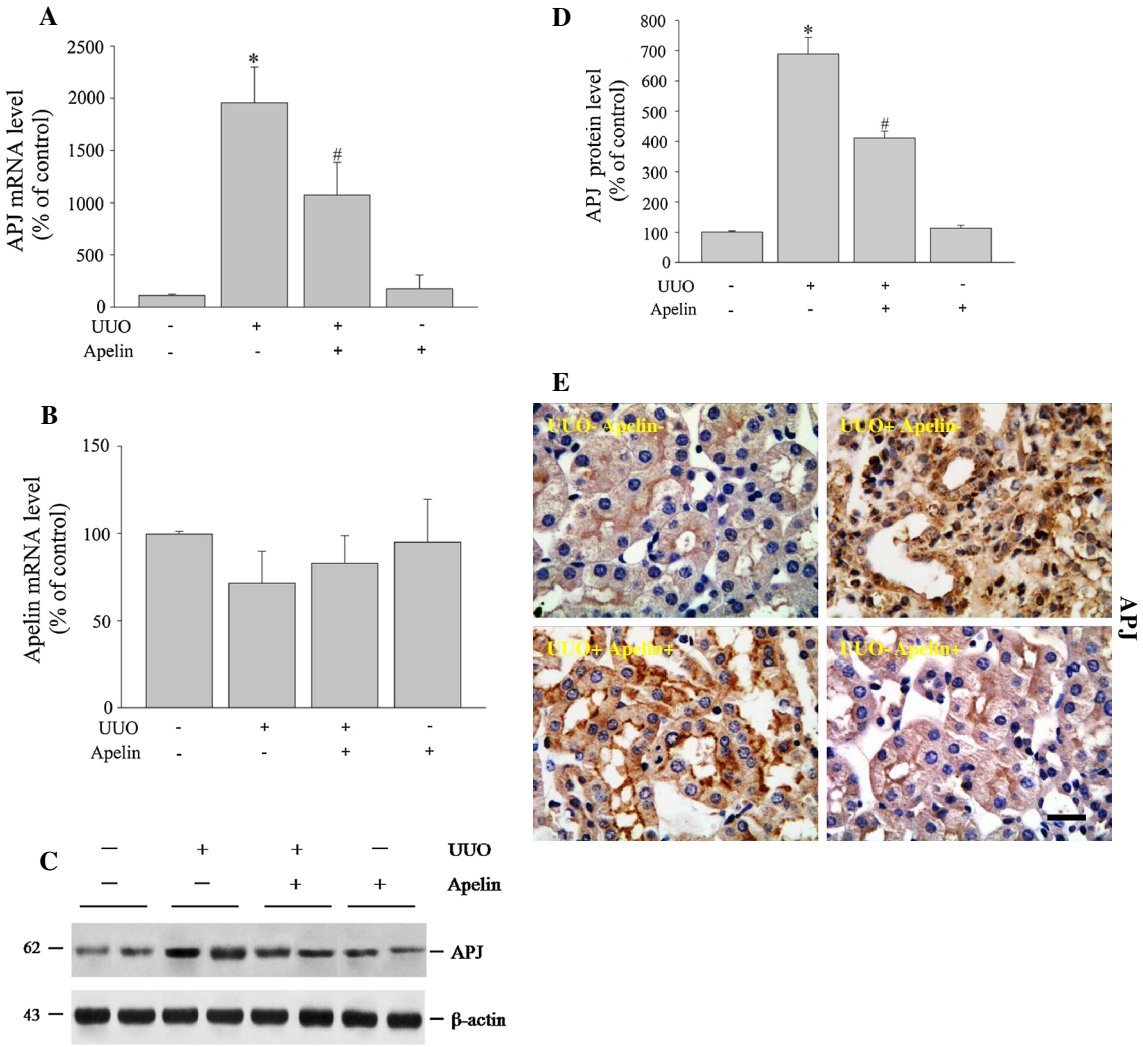

Fig. 7 Renal expression of APJ, but not apelin, is upregulated after ureteral obstruction. **a**, **b** Quantitative RT-PCR analysis demonstrated that the expression of APJ, but not apelin, was significantly increased in the ligated kidney at 14 days after UUO, and apelin-13 administration blunted this increase. GAPDH mRNA expression was used as an internal control. The dose of apelin-13 used was 0.1 μmol/kg body weight. **c**, **d** Western blotting and densitometric analysis of APJ protein levels in various groups. Kidney homogenates were immunoblotted with antibodies against APJ or β-actin. Results are presented as percentages of control values and are the means ± SD of five animals per group ($n = 5$). $^{*}P < 0.05$, compared with the UUO− apelin− group. $^{\#}P < 0.05$, compared with the UUO+ apelin− group. **e** Representative micrographs of immunohistochemical staining showing the expression and localization of APJ in the ligated kidney. *Scale bar* 20 μm

which maintain the normal morphology and functions of epithelial cells (Das et al. 2009; Kaneyama et al. 2010). In this context, the ability of apelin to attenuate the expression of α-SMA and restore the expression of E-cadherin in HK-2 cells, as shown in our study, underscores that apelin is effective for protection against tubular EMT. The inhibitory role of apelin in renal fibrosis was corroborated further by in vivo experiments. We used the UUO mouse model to induce tubulointerstitial lesions and fibrogenesis. Apelin prevented the transformation of epithelial cells and overproduction of interstitial matrix components in the renal parenchyma. Blocking experiments using an APJ antagonist F13A further demonstrated that apelin exerts renoprotective effects through its G protein-coupled APJ receptor.

However, the underlying mechanisms of apelin in the attenuation of the fibrotic process are unknown. As a regulatory peptide, apelin is derived from a precursor of 77 amino acids, which is processed to several isoforms, including apelin-36, apelin-17, and apelin-13, by modification of the amino terminus (Lu et al. 2012). In many in vitro and in vivo studies, apelin-13 is the most commonly used form because it has more pronounced biological effects. In terms of the relationship between apelin and fibrosis, there may be different

roles in various tissues. Apelin has been demonstrated to inhibit sphingosine kinase-1, an enzyme that induces collagen production in cardiac fibroblasts, and thus blocks ongoing fibrotic progression in the heart induced by pressure overload (Pchejetski et al. 2012). Similarly, another study has shown that apelin protects against cardiac fibrosis and vascular remodeling through synergistic inhibition of Ang II signaling and increased production of nitric oxide (Siddiquee et al. 2011). However, unlike the protective effects it plays in cardiovascular system, apelin behaves as an inducer in liver fibrosis as shown by selective hepatic activation of the apelinergic system in rats with cirrhosis, together with a decrease in fibrosis and neoangiogenesis resulting from administration of apelin receptor blockade (Principe et al. 2008). The inductive effects of apelin are mediated through promotion of collagen matrix synthesis in hepatic stellate cells and triggering of proinflammatory and neoangiogenic signaling pathways (Melgar-Lesmes et al. 2010). These findings indicate that the effects and mechanisms of apelin in the regulation of fibrotic processes are very complex and still controversial.

Previous studies have only described the regulatory function of apelin in normal kidneys. The apelinergic system is distributed all along the nephron. It acts on pre- and postglomerular microvasculature to regulate renal hemodynamics, and on the collecting duct to play an aquaretic role (Hus-Citharel et al. 2008). However, there are few reports describing how the apelinergic system responds and which roles it might play in kidney disease. It has been reported that pharmacological blockade of the Ang II/AT-1 system exerts some alleviative effects on renal fibrosis, which may be indirectly mediated by upregulation of the apelinergic system and activation of the Akt/eNOS pathway (Nishida et al. 2012). In the present study, we have demonstrated for the first time that treatment with apelin directly blocks the TGF-β1/Smad pathway in tubular EMT and renal fibrosis. TGF-β1 generally exerts signaling effects by activating its heteromeric receptors of two transmembrane serine/threonine kinases, type I and type II receptors (TβRI and TβRII) (Derynck and Zhang 2003). Activated TβRI triggers phosphorylation of the receptor-regulated Smad2/3. Phosphorylated Smad2/3 bind to Smad4, and then the activated complex translocates to the nucleus where it interacts with other transcriptional coactivators to regulate the expression of numerous genes for EMT induction (Ten and Hill 2004). The inhibitory Smad7 acts in a negative feedback loop to inhibit TGF-β1 activity by preventing phosphorylation and nuclear accumulation of Smad2/3 (Itoh and Ten 2007). In our study, we observed that apelin inhibited the TGF-β1-induced increase of phosphorylated Smad2/3 and decrease of Smad7 in vitro, and attenuated the upregulation of TβRI and its downstream Smad signaling in vivo. Although there are multiple signaling proteins in addition to Smads, which are implicated in the induction of EMT, the finding that apelin is able to target this key signaling pathway highlights a fundamental role of apelin in controlling tubular EMT, thereby vindicating its roles in renoprotection. Undoubtedly, elucidating the relative contribution of other pathways and their crosstalk with apelin for overall renal protection is necessary, but it remains a challenging issue that merits further investigation.

One striking observation in our study was the dramatic upregulation of APJ in TGF-β1-stimulated HK-2 cells and fibrotic kidneys, which was attenuated by exogenous supplementation of apelin. Conversely, we observed a decrease in the plasma level of apelin in UUO mice. We speculate that the increased expression of APJ in the injured kidney may represent a compensatory response to overcome the downregulation of plasmatic apelin and progression of renal fibrosis. Previous studies have revealed similar compensatory mechanisms of apelin/APJ in the cardiovascular system. It has been shown that the left ventricular mRNA level of apelin is upregulated in patients with heart failure caused by coronary heart disease or idiopathic dilated cardiomyopathy (Foldes et al. 2003). However, the levels of apelin/APJ in the cardiovascular system are not identical in various types and stages of cardiac pathologies (Falcao-Pires et al. 2009). There are also some findings that appear to be contradictory with our results. For example, APJ expression in kidneys is decreased in the diabetic or renal hypertension model (Najafipour et al. 2012; Day et al. 2013). We speculate that this discrepancy may be caused by the difference in the underlying renal pathophysiology. In CKD patients, there is a significant reduction in the plasma level of apelin, which may be attributed to the vascular endothelial dysfunction caused by uremic toxins (Codognotto et al. 2007). This observation can partly explain the cause of the decreased plasma level of apelin in UUO mice. Collectively, our results prompt a broader hypothesis of the antifibrotic renal protection of apelin. However, in various types and stages of CKD, which responses and roles the apelinergic system performs still warrant further studies.

In conclusion, we have demonstrated that apelin is able to protect against tubular EMT and renal fibrosis. The antifibrotic effects of apelin are mediated through antagonism of the TGF-β1/Smad pathway, resulting in decreased matrix collagen production and improved tubulointerstitial lesions. These data suggest that apelin behaves as a potential suppressor of renal profibrotic activity. Therefore, supplementation with exogenous apelin may be a promising strategy for slowing or halting the progression of CKD.

Acknowledgments This study received financial support from the National Natural Science Foundation of the People's Republic of China (81300607), the Beijing Natural Science Foundation (7132091), Beijing Municipal Science and Technology Commission Funds (D131100004713001; Z121107001012138), and Capital Health Research and Development Project (2011-2002-02).

Conflict of interest None declared.

References

Berry MF, Pirolli TJ, Jayasankar V et al (2004) Apelin has in vivo inotropic effects on normal and failing hearts. Circulation 110:II 187–II 193

Cayabyab M, Hinuma S, Farzan M et al (2000) Apelin, the natural ligand of the orphan seven-transmembrane receptor APJ, inhibits human immunodeficiency virus type 1 entry. J Virol 74:11972–11976

Codognotto M, Piccoli A, Zaninotto M et al (2007) Evidence for decreased circulating apelin beyond heart involvement in uremic cardiomyopathy. Am J Nephrol 27:1–6

Compagnone A, Bandino A, Meli F et al (2012) Polyamines modulate epithelial-to-mesenchymal transition. Amino Acids 42:783–789

Coresh J, Selvin E, Stevens LA et al (2007) Prevalence of chronic kidney disease in the United States. JAMA 298:2038–2047

Cui RR, Mao DA, Yi L et al (2010) Apelin suppresses apoptosis of human vascular smooth muscle cells via APJ/PI3-K/Akt signaling pathways. Amino Acids 39:1193–1200

Das S, Becker BN, Hoffmann FM, Mertz JE (2009) Complete reversal of epithelial to mesenchymal transition requires inhibition of both ZEB expression and the Rho pathway. BMC Cell Biol 10:94

Day RT, Cavaglieri RC, Feliers D (2013) Apelin retards the progression of diabetic nephropathy. Am J Physiol Renal Physiol 304:F788–F800

Derynck R, Zhang YE (2003) Smad-dependent and Smad-independent pathways in TGF-beta family signalling. Nature 425:577–584

El-Shehaby AM, El-Khatib MM, Battah AA, Roshdy AR (2010) Apelin: a potential link between inflammation and cardiovascular disease in end stage renal disease patients. Scand J Clin Lab Invest 70:421–427

Falcao-Pires I, Goncalves N, Henriques-Coelho T et al (2009) Apelin decreases myocardial injury and improves right ventricular function in monocrotaline-induced pulmonary hypertension. Am J Physiol Heart Circ Physiol 296:H2007–H2014

Foldes G, Horkay F, Szokodi I et al (2003) Circulating and cardiac levels of apelin, the novel ligand of the orphan receptor APJ, in patients with heart failure. Biochem Biophys Res Commun 308:480–485

He W, Dai C, Li Y et al (2009) Wnt/beta-catenin signaling promotes renal interstitial fibrosis. J Am Soc Nephrol 20:765–776

Hus-Citharel A, Bouby N, Frugiere A et al (2008) Effect of apelin on glomerular hemodynamic function in the rat kidney. Kidney Int 74:486–494

Itoh S, Ten DP (2007) Negative regulation of TGF-beta receptor/Smad signal transduction. Curr Opin Cell Biol 19:176–184

Jones LK, O'Sullivan KM, Semple T et al (2009) IL-1RI deficiency ameliorates early experimental renal interstitial fibrosis. Nephrol Dial Transplant 24:3024–3032

Kaneyama T, Kobayashi S, Aoyagi D, Ehara T (2010) Tranilast modulates fibrosis, epithelial–mesenchymal transition and peritubular capillary injury in unilateral ureteral obstruction rats. Pathology 42:564–573

Kawamata Y, Habata Y, Fukusumi S et al (2001) Molecular properties of apelin: tissue distribution and receptor binding. Biochim Biophys Acta 1538:162–171

Lan HY (2003) Tubular epithelial–myofibroblast transdifferentiation mechanisms in proximal tubule cells. Curr Opin Nephrol Hypertens 12:25–29

Li Y, Yang J, Dai C, Wu C, Liu Y (2003) Role for integrin-linked kinase in mediating tubular epithelial to mesenchymal transition and renal interstitial fibrogenesis. J Clin Invest 112:503–516

Liu Y (2004) Epithelial to mesenchymal transition in renal fibrogenesis: pathologic significance, molecular mechanism, and therapeutic intervention. J Am Soc Nephrol 15:1–12

Liu Y (2006) Renal fibrosis: new insights into the pathogenesis and therapeutics. Kidney Int 69:213–217

Lu Y, Zhu X, Liang GX et al (2012) Apelin-APJ induces ICAM-1, VCAM-1 and MCP-1 expression via NF-kappaB/JNK signal pathway in human umbilical vein endothelial cells. Amino Acids 43:2125–2136

Medhurst AD, Jennings CA, Robbins MJ et al (2003) Pharmacological and immunohistochemical characterization of the APJ receptor and its endogenous ligand apelin. J Neurochem 84:1162–1172

Melgar-Lesmes P, Casals G, Pauta M et al (2010) Apelin mediates the induction of profibrogenic genes in human hepatic stellate cells. Endocrinology 151:5306–5314

Najafipour H, Soltani HA, Nekooian AA, Esmaeili-Mahani S (2012) Apelin receptor expression in ischemic and non- ischemic kidneys and cardiovascular responses to apelin in chronic two-kidney-one-clip hypertension in rats. Regul Pept 178:43–50

Nishida M, Okumura Y, Oka T et al (2012) The role of apelin on the alleviative effect of Angiotensin receptor blocker in unilateral ureteral obstruction-induced renal fibrosis. Nephron Extra 2:39–47

Pchejetski D, Foussal C, Alfarano C et al (2012) Apelin prevents cardiac fibroblast activation and collagen production through inhibition of sphingosine kinase 1. Eur Heart J 33:2360–2369

Principe A, Melgar-Lesmes P, Fernandez-Varo G et al (2008) The hepatic apelin system: a new therapeutic target for liver disease. Hepatology 48:1193–1201

Siddiquee K, Hampton J, Khan S et al (2011) Apelin protects against angiotensin II-induced cardiovascular fibrosis and decreases plasminogen activator inhibitor type-1 production. J Hypertens 29:724–731

Sorhede WM, Magnusson C, Ahren B (2005) The apj receptor is expressed in pancreatic islets and its ligand, apelin, inhibits insulin secretion in mice. Regul Pept 131:12–17

Strutz FM (2009) EMT and proteinuria as progression factors. Kidney Int 75:475–481

Sun S, Ning X, Zhang Y et al (2009) Hypoxia-inducible factor-1alpha induces Twist expression in tubular epithelial cells subjected to hypoxia, leading to epithelial-to-mesenchymal transition. Kidney Int 75:1278–1287

Ten DP, Hill CS (2004) New insights into TGF-beta-Smad signalling. Trends Biochem Sci 29:265–273

Wynn TA (2008) Cellular and molecular mechanisms of fibrosis. J Pathol 214:199–210

Yang J, Liu Y (2002) Blockage of tubular epithelial to myofibroblast transition by hepatocyte growth factor prevents renal interstitial fibrosis. J Am Soc Nephrol 13:96–107

Zeisberg M, Hanai J, Sugimoto H (2003) BMP-7 counteracts TGF-beta1-induced epithelial-to-mesenchymal transition and reverses chronic renal injury. Nat Med 9:964–968